Original Paper

Landslides (2014) 11:969–979
DOI 10.1007/s10346-013-0457-6
Received: 24 December 2012
Accepted: 6 December 2013
Published online: 24 December 2013

Sho Kimura · Shinya Nakamura · Shriwantha Buddhi Vithana · Kazuhito Sakai

Shearing rate effect on residual strength of landslide soils in the slow rate range

Abstract In the present study, we investigate the influence of shearing rate on the residual strength parameters, ϕ_r, in landslide soils using ring-shear tests at two shearing rates (0.01 and 0.5mm/min) under selected effective normal stresses. The landslide soil samples used for this study cover a wide range of soil types and properties. Relationships between the ϕ_r and soil properties, such as liquid limit, plasticity index, and the clay fraction show that the ϕ_r decreases with increasing soil LL, I_p and CF. The differences in the ϕ_r at two shearing rates, $\phi_{r\ (0.5)}-\phi_{r\ (0.01)}$, under different effective normal stresses are either negative or positive values of which the maximum magnitude is generally about 1.0°. The relationships between the $\phi_{r\ (0.5)}-\phi_{r\ (0.01)}$ and the soil properties (LL, I_p, and CF) are not exhibited in a regular pattern. On the other hand, the $\phi_{r\ (0.5)}$ and $\phi_{r\ (0.01)}$ determined at each effective normal stress suggest that the tendency for increased negative effect of the ϕ_r with decreasing effective normal stress is more noticeable in the slow shearing rate range. The absolute value of $\phi_{r\ (0.5)}-\phi_{r\ (0.01)}$ at lower effective normal stress is found to be greater than 1.0°, with the maximum of about 4.0°. The negative shearing rate effect on ϕ_r at low effective normal stress is affected by the undulating shear behavior due to poor or no slickenside development.

Keywords Residual strength · Shearing rate · Ring-shear test · Slip surface soils

Introduction

Residual strength is an extremely important soil parameter from the viewpoint of stability of reactivated as well as first-time slides, when the potential sliding surface may develop along lithologic discontinuities and geological structural discontinuities such as sheared bedding-planes, joints, or faults. Residual strength is like to be mobilized on particle-oriented surfaces of soil and rock after large displacement (Skempton 1964, 1985; Mesri and Shahien 2003; Nakamura et al. 2010). A torsional ring-shear test apparatus is considered suitable for measuring the residual strength, as it essentially permits an infinite displacement (Bishop et al. 1971; Lupini et al. 1981; Skempton. 1985; Gibo et al. 1987; Stark and Eid 1997; Tiwari and Marui 2005; Meehan et al. 2010, 2011; Nakamura et al. 2010; Vithana et al. 2012a). In geotechnical literature, it has been reported that the shear behavior during the residual state may or may not vary with different shearing rates in natural soils or pure mineral soils (La Gatta 1970; Hungr and Morgenstern 1984; Skempton 1985; Lemos et al. 1985; Yatabe et al. 1991; Lehane and Jardine 1992; Tika et al. 1996; Tika 1999; Tika and Hutchinson 1999; Suzuki et al. 2000; Toyota et al. 2009; Grelle and Guadagno 2010; Wang et al. 2010a, b; Bhat et al. 2013). For example, Tika et al. (1996) showed that some soils exhibit a minimum strength that is greater than the residual strength (positive rate effect) when shearing at higher speed, while some soil exhibit a negative rate effect or a constant (neutral) rate effect (Fig. 1). Thus, as there is a possibility that differences in measured residual strength at different shearing rates could be encountered, the influence of the shearing rate on the residual strength should be carefully considered in the determination of the residual strength to obtain design parameters with high accuracy and reliability. The primary aim of this study is to investigate the variation of strength at the residual state.

Residual strength parameters (friction angle ϕ_r (cohesion c_r is zero)) of soil are essential for stability analysis and design of countermeasures against the reactivation of landslides. Residual strength parameters could be also used for evaluating the stability of the first-time landslides. Good understanding of residual strength parameters and their dependence on testing procedures might affect the net result of the stability assessment of landslides. Hungr and Morgenstern (1984), Yatabe et al. (1991) carried out high-velocity ring-shear tests on some sand material and found that the residual strength parameters were not influenced by the shearing rate. However, Tika (1999) suggested that the residual friction angle decreases with the increasing shearing rate on carbonate sandy silt samples. On the other hand, in the slow shearing rate range, Yokota et al. (1995, 1997) mentioned, without providing details, that shearing rates below 1.01 mm/min make little impact on residual strength parameters in the ring-shear tests. In contrast, Skempton (1985) showed that the change in residual strength below 1.0 mm/min is about 2.5 % per log cycle in ring-shear tests on two clay samples over a range of speeds from about 100 times slower to 100 times faster than the usual (slow) laboratory test rate. The shearing rate effect on the residual strength of landslide soil has not been sufficiently investigated even in the slow rate range. These conclusions lead to the fact that it is necessary to investigate the relationship between residual strength and shearing rate for various types of landslide soil samples in order to have a better understanding of the appropriate method of the residual strength testing in the slow shearing rate range. In addition, it is also important to understand the influence of the shearing rate on the residual strength parameters under a range of effective normal stresses, which has been shown to have an effect on the residual strength (Bishop et al. 1971; Hawkins and Privett 1985; Gibo et al. 1987; Nakamura et al. 1999).

In this study, we have examined the physical soil properties, such as liquid limit, plastic limit and quantified the clay, silt and sand fractions. The residual strength was tested at two different shearing rates. Soil samples were collected from various landslide sites. The main objective of this work is to investigate the degree of variation in the residual strength parameters of soil samples at different shearing rates and their relationship with the effective normal stress in the slow shearing rate range.

Experimental procedures

Landslide soil samples

Soil samples used for the ring-shear tests and laboratory index tests were collected from landslides in a disturbed condition by the authors. Fifteen samples, as shown in Table 1, have been collected from 12 landslides that have occurred in Japan, Chin,a and Taiwan.

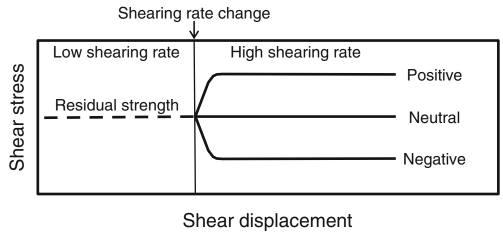

Fig. 1 Simple sketch of negative, positive and neutral rate effect in shear behavior

They differ in geological origin. Landslides particularities have been previously described in the literature: Kamenose (Yamaguchi 1980; Gibo et al. 1987), Odokoro (Egashira et al. 2000), Tyunjun (Nakamura et al. 2004), Asato (Kimura et al. 2009), Morikawa (Nakamura et al. 2011a), Erdaocha (Gibo et al. 2007), Ikeda, Arakawa (Gibo et al. 2009), Chenyoulanxi (Gibo et al. 1997), Miaowan (Sun et al. 2004), Yona and Izumi (Nakamura et al. 2011b). Soil samples were collected from the slip surface that was found in the borehole soil samples. Where no borehole samples were available, the soil sampling was done from the exposed scarp or toe of the landslide.

Soil samples were first air dried in the laboratory, hand-milled with a roller to disintegrate the aggregates and passed through the standard sub-0.425-mm sieve. Extreme caution was taken with the predominantly sandy samples to avoid crushing of the sand particles in the disintegration process prior to sieving.

Analysis of physical properties

The soil was separated according to particle size by passing through the 0.425 mm sieve. Material passing the 0.425 mm sieve size was subjected to physical properties analysis. Liquid and plastic limit analyses were performed according to the JIS A 1205 methods (Japanese Geotechnical Society 2000). A method described by Egashira et al. (2000) was employed to determine the grain size distribution. Each soil sample was first separated into clay (sub-0.002-mm), silt (0.002–0.02 mm), and sand (0.02–0.425 mm) fractions. During this process, the soil sample was treated with hot 7 % H_2O_2 to remove any organic matter, then dispersed using ultrasonic vibration, and finally deflocculated by adding a small amount of 1 M NaOH to adjust the pH of the suspension to 10. After the soil sample preparation, the clay fraction was completely separated by repetitive cycles of sonification, sedimentation, and siphoning. The silt fraction was also separated by repeated sedimentation and siphoning, leaving the sand fraction as sediment. Each fraction was then weighed to calculate the particle size distribution.

Measurement of residual strength

The measurement of the residual strength was performed by using a ring-shear test apparatus. Reconstituted samples of the sub-0.425-mm soil fraction were used in the testing program. The ring-shear apparatus used in this study was designed by Gibo (1994). A normal load is applied through a pneumatic system. The effective normal load on shear plane is recorded by a load cell under the ring-shear box. This method subtracts the side friction between the confining ring and soil specimen from the total applied normal load. The torque is measured below the ring-shear box to eliminate the ball bearing friction that occurs during rotary motion. The gap between the upper and lower of confining rings after completion of consolidation press can is kept opened to avoid ring-to-ring friction and to measure accurate shear stress of

Table 1 Physical properties of sub-0.425-mm soil fraction of landslide soils and average slope inclinations

No.	Sample	Geology	Grain size distribution (%)			Liquid limit (%)	Plasticity index	Average slope inclination (Degrees)
			Clay (sub-0.002-mm)	Silt (0.002–0.02 mm)	Sand (0.02–0.425 mm)	LL	I_P	
1	Erdaocha1	Shale, Cretaceous	81.8	16.4	1.8	122.1	78.4	10.7
2	Kamenose	Tuff, Neogene	73.2	17.8	9.0	114.0	64.0	2.1
3	Ikeda	Mudstone, Neogene	66.6	29.1	4.4	66.1	40.5	21.0
4	Morikawa	Mudstone, Neogene	66.2	28.6	5.2	69.3	46.6	27.9
5	Asato	Mudstone, Neogene	64.5	29.7	5.8	72.3	48.8	8.5
6	Arakawa	Mudstone, Neogene	63.6	30.8	5.6	62.7	30.9	20.7
7	Miaowan2	Alluvial loess, Quaternary	62.2	28.2	9.6	41.9	19.9	10.7
8	Miaowan1	Siltstone, Paleogene	58.6	25.0	16.4	42.5	23.8	10.7
9	Yona	Phyllite, Mesozoic	57.9	32.6	9.5	34.3	19.2	25.5
10	Tyunjun	Mudstone, Neogene	57.9	37.8	4.3	80.0	57.1	12.0
11	Odokoro	Silicified shale, Paleozoic	50.8	20.7	28.5	-	14.5	
12	Izumi	Phyllite, Mesozoic	47.5	41.0	11.5	42.2	16.7	29.2
13	Chenyoulanxi	Shale, Pre-Tertiary	35.3	31.4	33.3	27.0	10.8	26.0
14	Erdaocha2	Malan loess, Quaternary	29.7	34.7	35.6	34.3	16.1	10.7
15	Miaowan3	Malan loess, Quaternary	18.7	30.9	50.4	31.3	12.5	10.7

soils during the shearing. The apparatus with a similar concept to the one described above has also been used in other previous studies (Zhou et al. 1997; Nakamura and Gibo 2000; Nakamura et al. 2000; Nakamura 2001; Gibo et al. 2002; Toyota et al. 2009; Nakamura et al. 2010; Vithana et al. 2012a, b). The ring-shear apparatus shears a specimen in a uni-directional, rotational movement for unlimited relative displacement. The application and maintenance of effective normal stress, shearing rate, and data retrieval are computer controlled. The measurement features of the ring-shear test apparatus used in this study are described in the following; maximum normal stress of 1,000 kN/m², shearing rate range of 0.001 to 10 mm/min, data acquisition system simultaneously with digital indicator and desk top computer, accuracy range for the data acquisition: normal stress 0.03 kN/m², shear stress 0.008 kN/m², vertical displacement: 0.0025 mm, and rotation 0.005°.

The ring-shear test is the preferred method compared to other shear tests because it can better accommodate large displacement that is more representative for a landslide movement. Reconstituted specimens were used based on the contention that the residual strength is unaffected by the initial soil structure (La Gatta 1970; Bishop et al. 1971; Stark et al. 2005; Vithana et al. 2012b).

The torsional ring-shear test procedures used in this study complies with the ASTM D6467 guidelines (ASTM 2006). The soil sample in a form of slurry was poured into an annular shear ring with 100 and 60 mm outer and inner diameters, respectively. The soil slurry was then vertically consolidated under the incremental increase of effective normal stress until the required consolidation was achieved. The final height of the specimen in ring after the consolidation varied but was typically about to 20 mm. The specimen is sheared by rotating the lower half of the shear box, while the upper half remains stationary. From the fully softened state to the residual state, failure was induced on a horizontal plane at the boundary between the upper and lower confining rings, where a few-micrometer-wide gap is left open to avoid metal to metal friction during shearing. An ideal gap size would satisfy the demand of no soil leakage during the consolidation and only a slight or no soil leakage during the shearing.

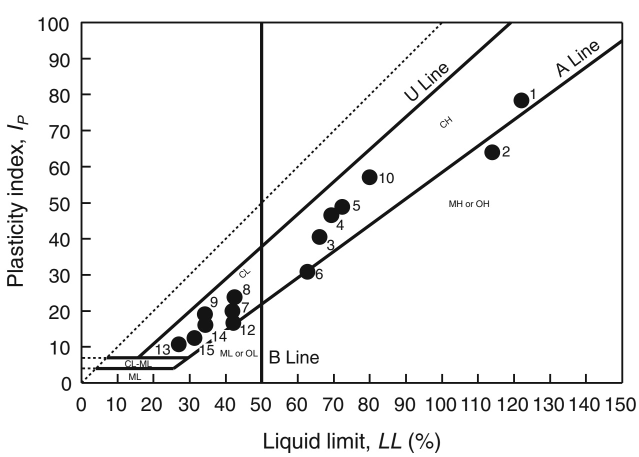

Fig. 2 Plasticity of the soil samples plotted on plasticity chart (based on Holtz and Kovacs 1981)

The soil samples were consolidated at different effective normal stresses ranging from 30 to 400 kN/m². In each test, the effective normal stress at the shearing was the same as consolidation pressure, giving the value of OCR of 1. Samples were subjected to shear while being submerged in deionized water until the residual state was attained. The ring-shear tests were performed under constant effective normal stress and drained condition during shearing. A single-stage shear test was performed under drained conditions. After performing the shear tests, soil sample was removed and remolded for the next shear tests under the next effective normal stress. From consolidation to the end of a complete shear test under a given effective normal stress, considerable time was required to reach residual conditions. For example, in a shear test at an effective normal stress of 50 kN/m², the incremental consolidation phase

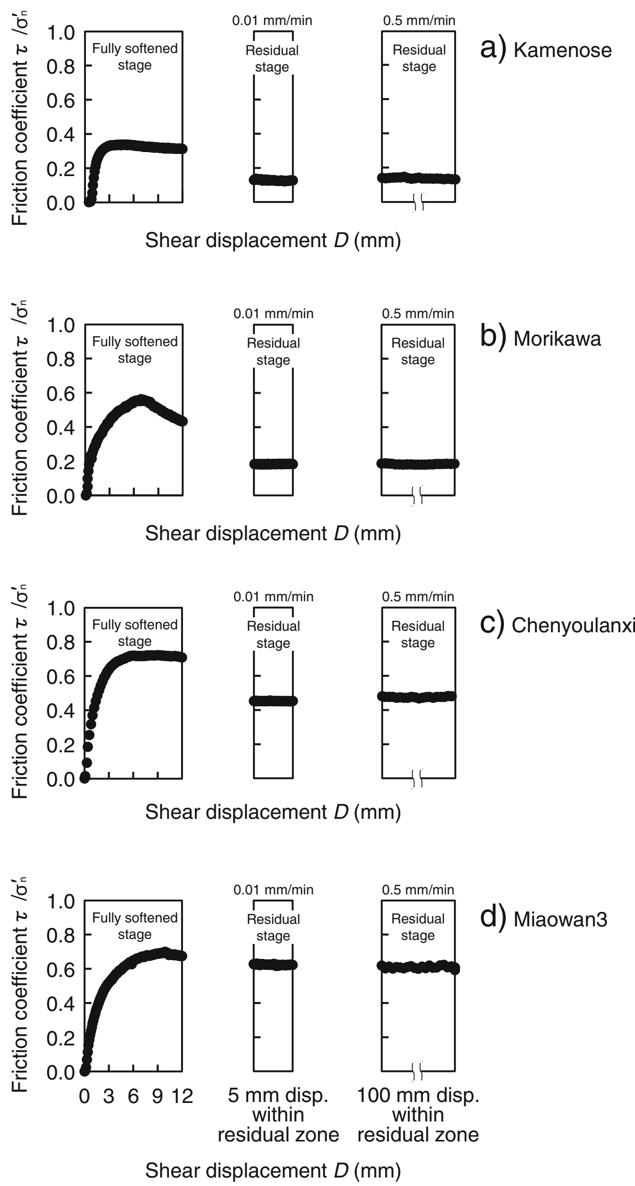

Fig. 3 Shear characteristics of the fully softened and residual stages for representative soil samples at 300 kN/m²

took at least 5 days. If the displacement required to achieve residual conditions is 150 mm (the recorded minimum and maximum displacements in this study were about 150 and 1,500 mm, respectively), it took another 11 days to complete the test using a shearing rate of 0.01 mm/min. The residual condition and the residual strength under each effective normal stress were determined by the minimum friction coefficient achieved at steady state. The shearing rates of 0.01 and 0.5 mm/min were used for the determination of the residual strength under various effective normal stresses. The rate of 0.01 mm/min and rate of 0.5 mm/min are classified as "Slow" and "Moderate" shearing rates, respectively as described by Tika et al. (1996), and they are referred as the "low" and the "high" rates described in this text.

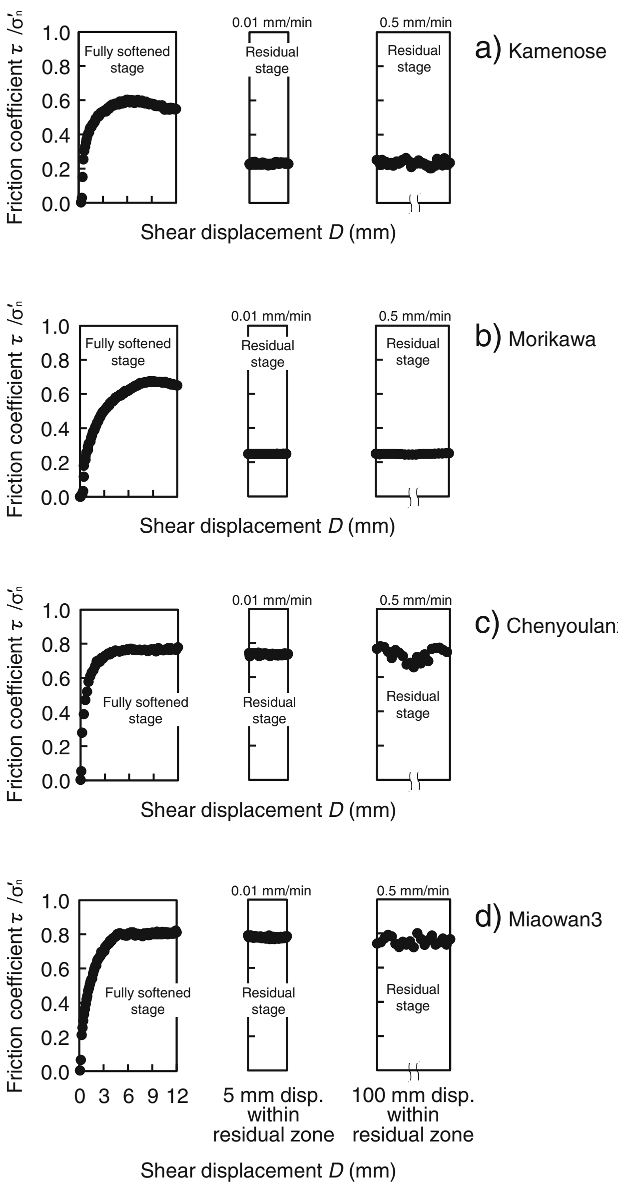

Fig. 4 Shear characteristics of the fully softened and residual stages for representative soil samples at 50 kN/m^2

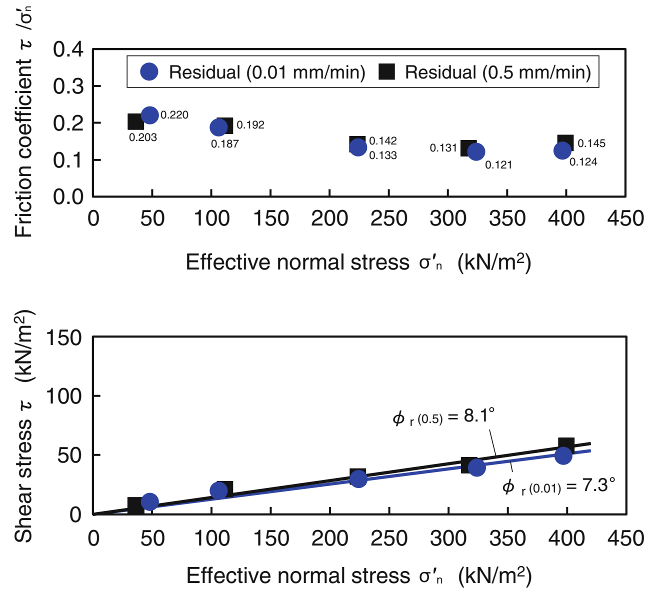

Fig. 5 Relationship between friction coefficient and effective normal stress, and residual strength parameter for Kamenose soil sample

Test program and results discussion

Physical properties of soil samples

Table 1 summarizes the physical properties of the sub-0.425-mm fraction soil samples. Samples significantly vary in the geological origin, which include tuff, shale, mudstone, silt stone, phyllite, etc. The clay fraction, CF (sub-0.002-mm), silt fraction (0.002–0.02 mm), sand fraction (0.02–0.425 mm), liquid limit, LL and plasticity index, I_P, of the samples varied between 18.7–81.8 %, 16.4–41.0 %, 1.8–50.4 % and 27.0–122.1 %, 10.8–78.4, respectively. The LL of Erdaocha 1 (No. 1)

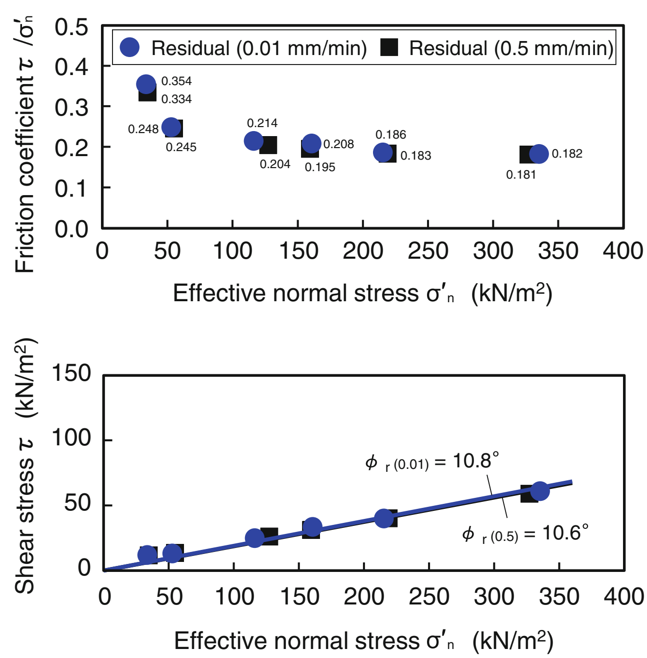

Fig. 6 Relationship between friction coefficient and effective normal stress, and residual strength parameter for Morikawa soil sample

and Kamenose (No. 2) had the highest LL of 122.1 and 114.0 %, respectively. The LL of mudstone samples is over 50 %. The lower group of LL is below about 40 %. The higher group of I_P among the samples was over around 50, while the lower I_P is about 10.

Figure 2 shows that the Atterberg limits of all samples fall into the common clay mineral group in the Casagrande plasticity chart (Holtz and Kovacs 1981). Most samples classify as high or low clay (CH or CL) according to the Unified Soil Classification System (USCS), with A, B, U lines.

Shear behavior

Figures 3 and 4 show the typical shear behavior characteristics of the fully softened and two different residual stages (shearing rate 0.01 and 0.5 mm/min) of four samples, where, the friction coefficient, τ/σ_n', is plotted against the shear displacement, D, at the effective normal stresses of 300 and 50 kN/m². The Kamenose (No. 2), Morikawa (No. 5), Chenyoulanxi (No. 14) and Miaowan3 (No. 13) samples were selected for having a wide range of clay fraction (18.7 to 73.2 %) and a liquid limit between 27.0 and 114.0 %. The residual strength of landslide soils is controlled by the soil properties such as clay fraction, consistency limits, clay mineralogy, and magnitude of effective normal stress.

At the effective normal stresses of 300 kN/m², the Kamenose and Morikawa samples showed over a 50 % decrease in the friction coefficient from the fully softened friction coefficient, which is greater than in the Chenyoulanxi (about 30 %) and Miaowan3 (about 10 %) samples. The fully softened strength here is the peak strength at normally consolidated condition. The minimum and maximum shear displacement required to achieve the residual conditions from the start of shear were 150 and 1,500 mm, respectively. In the Kamenose and Morikawa samples, a well-defined slickenside was clearly observed on the shear surface. This indicates a high degree of reorientation of clay particles induced by displacement during shearing. In Fig. 3a, b, it is noted that the decrease of the friction coefficient from the fully softened to the residual state in the Kamenose and Morikawa samples were over 50 % even for the samples consolidated at an effective normal stress of 50 kN/m² (Fig. 4a, b), while, the friction coefficient reduction in Chenyoulanxi and Miaowan3 samples were equivalent to only about 5 and 10 %. The Chenyoulanxi and Miaowan3

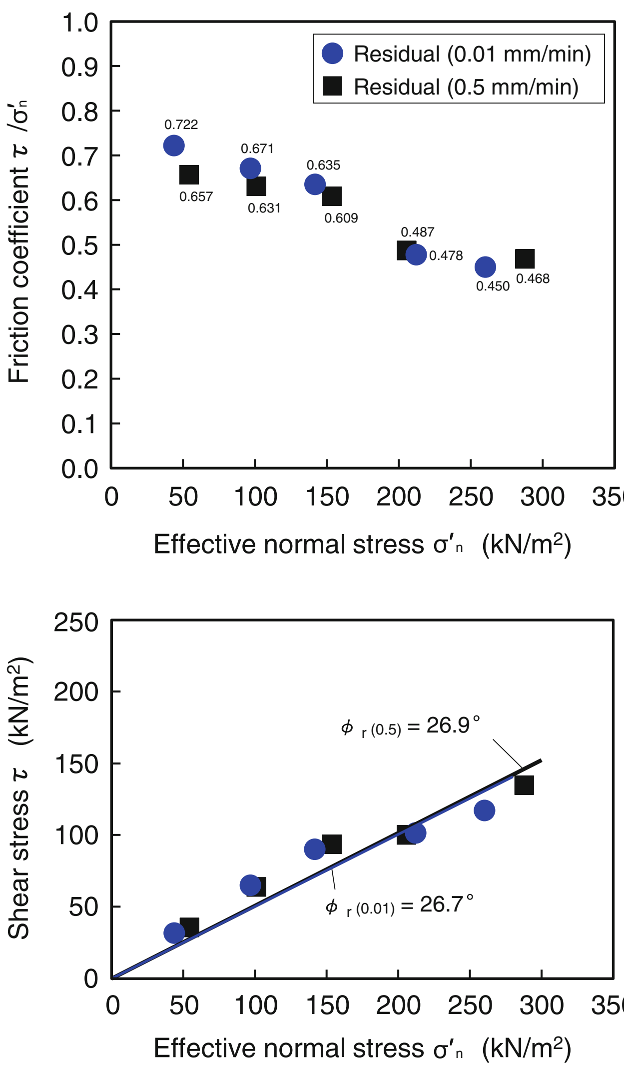

Fig. 7 Relationship between friction coefficient and effective normal stress, and residual strength parameter for Chenyoulanxi soil sample

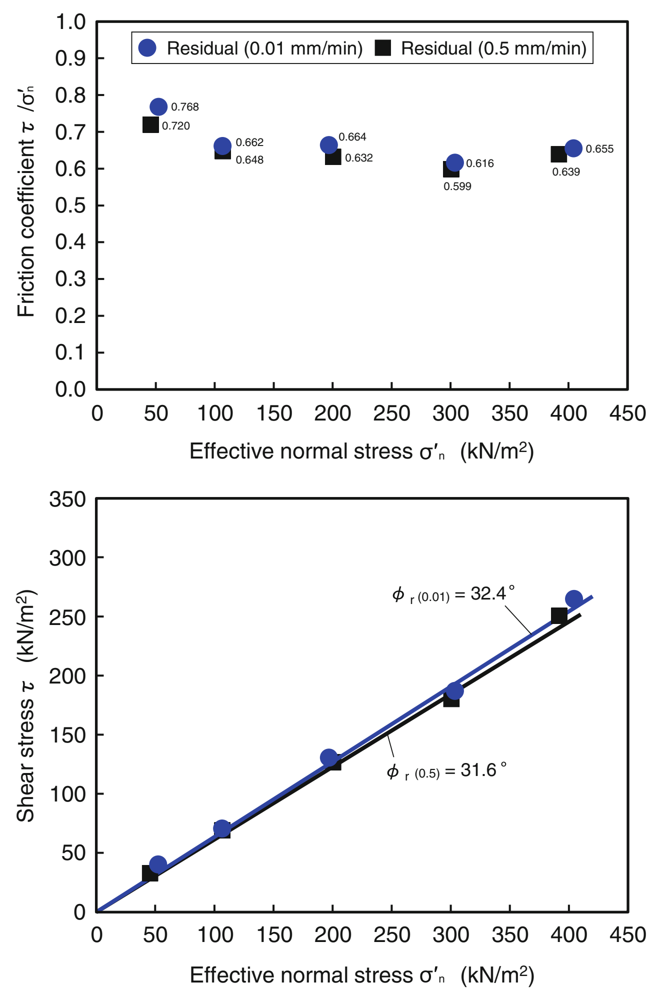

Fig. 8 Relationship between friction coefficient and effective normal stress, and residual strength parameter for Miaowan3 soil sample

Table 2 Residual strength parameters of sub-0.425-mm soil fraction of landslide soils

No.	Sample	Effective normal stress after consolidation σ_n' (kN/m^2)	Residual strength parameter				Difference in parameter $\phi_{r\ (0.5)}-\phi_{r\ (0.01)}$ (Degrees)	
			0.01 mm/min $\phi_{r\ (0.01)}$ ($c_{r\ (0.01)}=0$) (Degrees)		0.5 mm/min $\phi_{r\ (0.5)}$ ($c_{r\ (0.5)}=0$) (Degrees)			
			Under each σ_n'	Under all σ_n'	Under each σ_n'	Under all σ_n'	Under each σ_n'	Under all σ_n'
1	Erdaocha1	47.4	18.1	10.7	15.2	10.4	−2.9	−0.3
		188.8	10.7		10.1		−0.6	
		290.7	10.6		10.4		−0.2	
2	Kamenose	46.4	12.4	7.3	11.5	8.1	−0.9	+0.8
		91.6	10.6		10.8		+0.2	
		205.0	7.6		8.1		+0.5	
		293.1	6.9		7.5		+0.6	
		357.3	7.1		8.2		+1.1	
3	Ikeda	26.9	18.0	12.0	14.2	11.3	−3.8	−0.7
		92.3	14.2		12.1		−2.1	
		281.2	11.6		11.1		−0.5	
4	Morikawa	29.2	19.5	10.8	18.5	10.6	−1.0	−0.2
		53.4	13.9		13.7		−0.2	
		101.4	12.1		11.5		−0.6	
		150.2	11.8		11.0		−0.8	
		206.5	10.5		10.4		−0.1	
		300.2	10.3		10.2		−0.1	
5	Asato	65.3	16.3	10.5	15.4	10.4	−0.9	−0.1
		200.9	11.2		10.8		−0.4	
		294.6	10.0		10.0		0.0	
6	Arakawa	99.3	18.4	14.4	18.2	14.0	−0.2	−0.4
		206.5	15.1		14.5		−0.6	
		305.5	13.7		13.3		−0.4	
7	Miaowan2	50.2	30.9	25.3	30.6	25.3	−0.3	0.0
		95.9	26.5		26.6		0.0	
		194.8	25.6		25.7		+0.1	
		305.4	24.9		24.9		0.0	
8	Miaowan1	57.6	31.8	28.1	31.8	27.6	0.0	−0.5
		98.9	29.2		27.8		−1.4	
		307.4	27.9		27.5		−0.4	
9	Yona	58.6	27.0	21.8	27.3	22.4	+0.3	+0.6
		109.1	23.9		24.4		+0.5	
		223.2	22.3		22.9		+0.6	
		312.2	21.2		21.7		+0.5	
10	Tyunjun	55.1	11.9	9.0	10.3	8.5	−1.6	−0.5
		93.1	9.6		8.3		−1.3	
		198.7	8.8		8.5		−0.3	
		286.2	8.9		8.5		−0.4	
11	Odokoro	49.5	14.6	9.9	14.5	10.3	−0.1	+0.4
		104.0	12.4		13.0		+0.6	

Table 2 (continued)

No.	Sample	Effective normal stress after consolidation $\sigma_n{}'$ (kN/m^2)	Residual strength parameter 0.01 mm/min $\phi_{r\ (0.01)}$ ($c_{r\ (0.01)}=0$) (Degrees) Under each $\sigma_n{}'$	Under all $\sigma_n{}'$	0.5 mm/min $\phi_{r\ (0.5)}$ ($c_{r\ (0.5)}=0$) (Degrees) Under each $\sigma_n{}'$	Under all $\sigma_n{}'$	Difference in parameter $\phi_{r\ (0.5)}-\phi_{r\ (0.01)}$ (Degrees) Under each $\sigma_n{}'$	Under all $\sigma_n{}'$
		150.3	10.8		11.6		+0.8	
		298.4	9.8		10.4		+0.6	
		421.7	9.6		9.7		+0.1	
12	Izumi	30.6	36.5	28.7	36.5	29.3	0.0	+0.6
		52.0	34.3		34.3		0.0	
		205.7	28.2		28.8		+0.6	
13	Chenyoulanxi	41.4	35.8	26.7	33.3	26.9	−2.5	+0.2
		95.2	33.8		32.2		−1.6	
		148.3	32.4		31.3		−1.1	
		183.4	25.5		25.9		+0.4	
		288.0	24.2		25.1		+0.9	
14	Erdaocha2	54.2	35.7	31.5	34.4	31.1	−1.3	−0.4
		106.1	35.7		34.6		−1.1	
		304.4	30.9		30.6		−0.3	
15	Miaowan3	47.3	37.5	32.4	35.7	31.6	−1.8	−0.8
		102.0	33.5		32.9		−0.6	
		202.0	33.6		32.3		−1.3	
		297.9	31.6		30.9		−0.7	
		391.3	33.2		32.6		−0.6	

soil samples could not easily be separated along the shear surface after the shear test was complete.

A stable shear behavior under two shearing rates at 300 kN/m^2 can even be found in sample with a high residual friction coefficient, i.e., silty/sandy (granular) soil sample (Fig. 3c, d). In contrast, under two shearing rates at 50 kN/m^2, although a stable shear behavior can be found in high clay content (cohesive) samples (Fig. 4a, b), an undulating shear behavior could be observed in samples with a high residual friction coefficient (Fig. 4c, d). This indicates that clay particles were poorly reoriented even after the large displacement shear because of a low clay content and plasticity.

Relationship between residual friction coefficient and effective normal stress, and residual strength parameters

For the four samples described above, that are considered as representative samples, Figs. 5, 6, 7, and 8 show the relationship between the friction coefficient, $\tau/\sigma_n{}'$, and the effective normal stress, $\sigma_n{}'$, and the residual strength parameters. The friction coefficient, $\tau/\sigma_n{}'$, is plotted against the effective normal stress, $\sigma_n{}'$, for the residual friction coefficients, $\tau_r/\sigma_n{}'$. The residual friction coefficient corresponds to the minimum value, which is measured during the residual stage at low and high shearing rates under all effective normal stresses. The strength parameters in residual stages are estimated by Coulomb's law of friction. Cohesion, c, was assumed to be zero by the method described by Skempton (1964, 1985). The residual friction coefficients at shearing rate of 0.01 and 0.5 mm/min were defined as $\tau_r/\sigma_n{}'(0.01)$ and $\tau_r/\sigma_n{}'(0.5)$, respectively. The residual strength parameter was defined as $\phi_{r\ (0.01)}$ at the low shearing rate and $\phi_{r\ (0.5)}$ at the high shearing rate, respectively. The difference between the friction coefficients and between the residual friction angles at two shearing rates were defined as $\tau_r/\sigma_n{}'(0.5)-\tau_r/\sigma_n{}'(0.01)$ and $\phi_{r\ (0.5)}-\phi_{r\ (0.01)}$, respectively.

Figure 5 shows that in the Kamenose sample (No. 2) the residual friction coefficients were low. The coefficients $\tau_r/\sigma_n{}'(0.01)$ and $\tau_r/\sigma_n{}'(0.5)$ at the effective normal stress of 50 to 400 kN/m^2 ranged from 0.220 to 0.121 and from 0.203 to 0.131, respectively. The difference between the friction coefficients, $\tau_r/\sigma_n{}'(0.5)-\tau_r/\sigma_n{}'(0.01)$, at each effective normal stress ranged from −0.017 to +0.020. As for the residual friction angle, $\phi_{r\ (0.5)}-\phi_{r\ (0.01)}$ ranged from −0.9 to +1.1°. For effective normal stresses above and including 100 kN/m^2, the coefficient $\tau_r/\sigma_n{}'(0.01)$ was smaller in magnitude than the coefficient $\tau_r/\sigma_n{}'(0.5)$. On the other hand, the coefficient $\tau/\sigma_n{}'(0.01)$ under the effective normal stress of 50 kN/m^2 was observed to be slightly greater than 0.017. Skempton (1985) and Gibo et al. (1987) concluded that the reorientation of clay particles and platy clay minerals parallel to the direction of shearing is an important factor influencing the residual strength. From this point of view, the difference in the residual friction coefficients while subjected to different shearing rates could be related to an underdeveloped shear surface at the residual stage under the low effective normal stress of 50 kN/m^2.

Figure 6 shows the results of the Morikawa sample (No. 4). The coefficients $\tau_r/\sigma_n{}'(0.01)$ and $\tau_r/\sigma_n{}'(0.5)$ at an effective normal stress of 30 to 300 kN/m^2 were 0.354 to 0.182 and 0.334 to 0.181, respectively. The difference $\tau_r/\sigma_n{}'(0.5)-\tau_r/\sigma_n{}'(0.01)$ at each effective normal stress ranged from −0.020 to −0.001, and the difference $\phi_{r\,(0.5)}-\phi_{r\,(0.01)}$ ranged from −1.0 to −0.1°. For this sample, residual friction coefficients show a slight decrease with the increasing shearing rate for all effective normal stress levels. The maximum difference was noted at the lowest effective normal stress of 30 kN/m^2.

Figure 7 presents the relationship in the Chenyoulanxi sample (No. 13). The coefficients $\tau_r/\sigma_n{}'(0.01)$ and $\tau_r/\sigma_n{}'(0.5)$ at 50 to 300 kN/m^2 were in range from 0.722 to 0.450 and from 0.657 to 0.468, respectively. The difference $\tau_r/\sigma_n{}'(0.5)-\tau_r/\sigma_n{}'(0.01)$ at each effective normal stress ranged from −0.064 to +0.018. The difference $\phi_{r\,(0.5)}-\phi_{r\,(0.01)}$ ranged from −2.5 to +0.9°. For the effective normal stress of 150 kN/m^2, the coefficient $\tau_r/\sigma_n{}'(0.5)$ was smaller than $\tau_r/\sigma_n{}'(0.01)$, while $\tau_r/\sigma_n{}'(0.5)$ again increased under higher effective normal stresses of 200 kN/m^2.

Figure 8 presents the relationship in the Miaowan3 sample (No. 15). The coefficients $\tau_r/\sigma_n{}'(0.01)$ and $\tau_r/\sigma_n{}'(0.5)$ at the effective normal stress of 50 to 400 kN/m^2 were in range from 0.768 to 0.616 and from 0.720 to 0.599, respectively. The difference $\tau_r/\sigma_n{}'(0.5)-\tau_r/\sigma_n{}'(0.01)$ at each effective normal stress ranges from −0.048 to −0.015. The difference $\phi_{r\,(0.5)}-\phi_{r\,(0.01)}$ ranges from −1.8 to −0.6°. The maximum difference in the residual friction angle of −1.8° was noted for the low effective normal stress of 50 kN/m^2. The residual friction coefficient seemed to have a decreasing tendency with the increasing shearing rate under all effective normal stresses.

The differences in the residual friction coefficient of each soil sample depending on the shearing rate had a connection with the effective normal stress. This is related to the difference in the development/formation of particle reorientation along the shear surface (Gibo et al. 1987).

The residual strength parameter $\phi_{r\,(0.01)}$ and $\phi_{r\,(0.5)}$ through all effective normal stresses were obtained to be 7.3° and 8.1°, respectively, for the Kamenose sample which is cohesive material (Fig. 5). The residual friction angles $\phi_{r\,(0.01)}$ and $\phi_{r\,(0.5)}$ of the Morikawa sample were of low values, 10.8° and 10.6°, respectively, while in the Chenyoulanxi sample $\phi_{r\,(0.01)}$ and $\phi_{r\,(0.5)}$ were high values, 26.7° and 26.9°, respectively (Figs. 6 and 7). The residual friction angles $\phi_{r\,(0.01)}$ and $\phi_{r\,(0.5)}$ of 32.4° and 31.6° were obtained for the Miaowan3 sample, which is a granular material (Fig. 8). Table 2 summarizes $\phi_{r\,(0.01)}$ and $\phi_{r\,(0.5)}$ of all samples obtained by the ring-shear tests. The residual friction angles $\phi_{r\,(0.01)}$ and $\phi_{r\,(0.5)}$ under all effective normal stresses ranged from 7.3 to 32.4° and from 8.1 to 31.6°, respectively.

The difference $\phi_{r\,(0.5)}-\phi_{r\,(0.01)}$ in the Kamenose and Miaowan3 samples, which is the effect of the shearing rate, were +0.8° and −0.8°, respectively. Yokota et al. (1995, 1997) reported that shearing rates below 1.01 mm/min do not affect residual strength in ring-shear tests. However, it is shown that the $\phi_{r\,(0.5)}-\phi_{r\,(0.01)}$ under all effective normal stresses were either negative or positive values of which the maximum magnitude was generally about 1.0°.

Effect of shearing rate on residual strength parameter based on soil properties

Figure 9 shows the variation in residual strength parameter at low and high shearing rates under all effective normal stresses as functions of soil properties such as liquid limit, plasticity index, and clay fraction. The residual friction angles $\phi_{r\,(0.01)}$ and $\phi_{r\,(0.5)}$ were found to decrease with increasing LL over 60 %. However, no relationship between ϕ_r at two deferent shearing rates and LL below 50 % was found. The relationship can agree with the residual friction angle correlation reported by Stark et al. (2005). In the relationship between ϕ_r and plasticity index, if the I_P is over 30, the ϕ_r at two deferent shearing rates gradually decrease from 15 to 7° with increasing I_P. The residual friction angles ϕ_r obtained at both shearing rates abruptly decreases from 30 to 10° with increasing I_P up to I_P=30. The residual friction angles ϕ_r of precipitous and gradational decrease with the increasing I_P in this study has been similar to the correlation of ϕ_r and I_P that was depicted by Kanji (1974), Mesri and Shahien (2003) using the data of Stark and Eid (1994, 1997). The residual friction angles ϕ_r for both shearing rates tend to decrease with the increasing CF. Data points were considered in three groups (below 50 %, 50–70 %, and over 70 % of CF). When the CF is below 50 %, the ϕ_r gradually decreases with

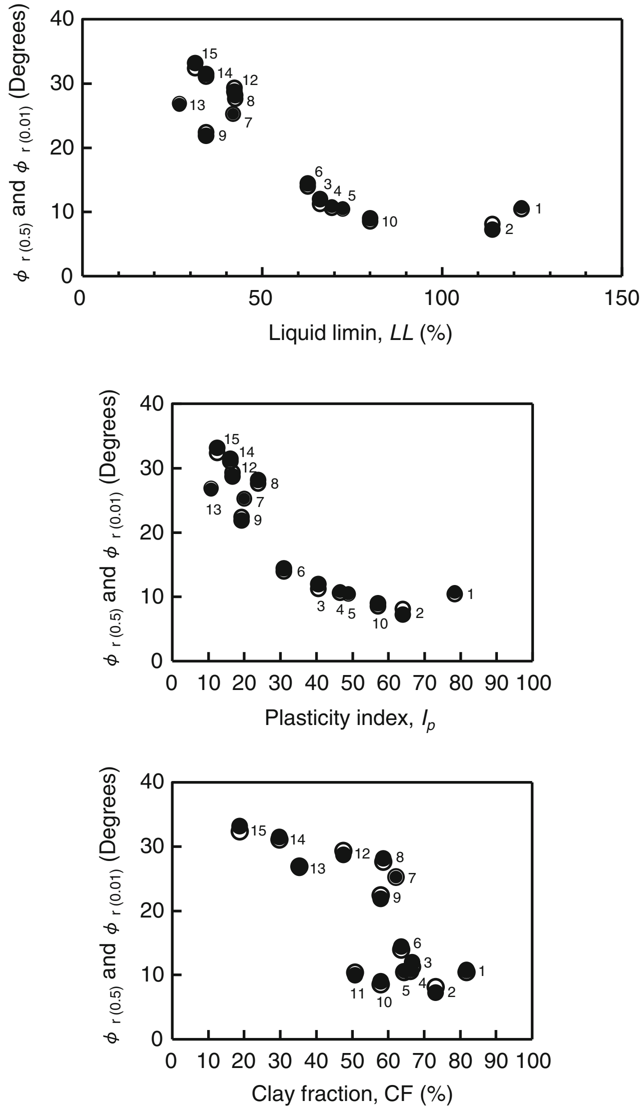

Fig. 9 Variation in residual strength parameter under 0.01 mm/min (*solid symbols*) and 0.5 mm/min (*open symbols*) as function of soil properties

increasing CF while it sharply decreases from about 30 to about 10° with increasing CF in the 50–70 % CF range. In the CF>70 %, the ϕ_r is almost constant at about 10°. The regions of three groups on the graph have been roughly equivalent to turbulent, transitional, and sliding shears, respectively, described by Lupini et al. (1981) and Skempton (1985). In Lupini's study, three similar regions on a graph are observed in the relationship between ϕ_r and the sub-0.002-mm clay fraction content for an artificially prepared sand-bentonite mixture having a series of mixing ratios.

Figure 10 depicts the variation in difference of residual strength parameter at "high" and "low" shearing rates ($\phi_{r\ (0.5)}-\phi_{r\ (0.01)}$) under all effective normal stresses in relation to some soil index properties (LL, I_P, CF). The absolute value of maximum $\phi_{r\ (0.5)}-\phi_{r\ (0.01)}$ was shown as smaller than 1.0° through the soil samples with varied soil properties. In the relationship between $\phi_{r\ (0.5)}-\phi_{r\ (0.01)}$ and CF, if the two soil groups are separated at CF of 50 % as clay (cohesive) and sandy (granular) soil groups, it is possible to see a pattern of increasing $\phi_{r\ (0.5)}-\phi_{r\ (0.01)}$ with increasing CF in the granular group where the CF is less than 50 %.

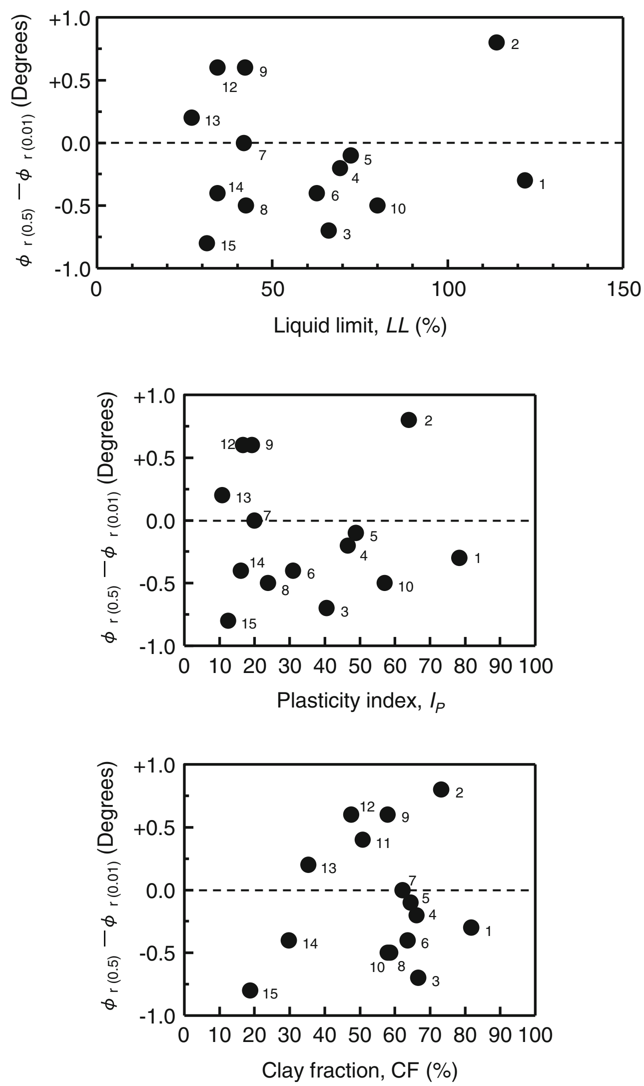

Fig. 10 Variation in difference of residual strength parameter under two shearing rate against soil properties

Influence of effective normal stress on shearing rate effect of residual strength parameter

The residual friction angles $\phi_{r\ (0.01)}$ and $\phi_{r\ (0.5)}$ of all samples obtained under each effective normal stress, with $c_r=0$, ranging from 6.9 to 37.5° and 7.5 to 36.5°, respectively, are shown in Table 2. The variation in the difference in the residual strength parameter at two different shearing rates under each effective normal stress as a function of clay fraction is shown in Fig. 11. The residual friction angles ϕ_r were determined at each effective normal stress from 30 to 400 kN/m² (Table 2). At effective normal stress less

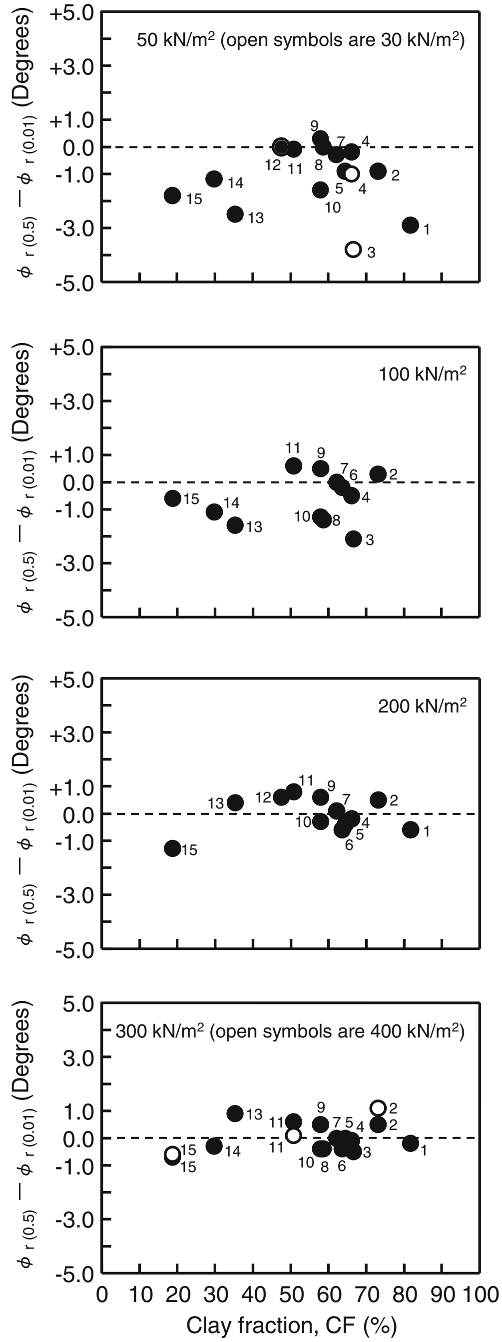

Fig. 11 Variation in difference residual strength parameter under two shearing rate at each of effective normal stress as a function of clay fraction

than or equal to 50 kN/m², equal to 100 kN/m², equal to 200 kN/m², and greater than or equal to 300 kN/m², the difference $\phi_{r\ (0.5)}-\phi_{r\ (0.01)}$ ranged from −3.8 to 0.3°, −2.1 to 0.6°, −1.3 to 0.8° and −0.7 to 1.1°, respectively. Average of $\phi_{r\ (0.5)}-\phi_{r\ (0.01)}$ at the above effective normal stress are −1.1°, −0.6°, 0.0°, and 0.0°, respectively. It is anticipated that the shearing rate effect on ϕ_r can be seen to increase with the decreasing effective normal stress. The tendency for increased negative effect on ϕ_r and for decreased positive effect of ϕ_r with the decreasing effective normal stress is apparent than in Fig. 11. An interesting point is that the shearing effect on ϕ_r has changed due to the magnitude of effective normal stress. This is observed in the soil behaviors during shearing in Figs. 3 and 4. At high effective normal stress, the stable shear behavior, controlled by slickenside reflected by high reorientation of particles on shear zone, is shown even for low plasticity soils in Fig. 3. In contrast, at lower effective normal stress the undulating shear behavior due to poor or no slickenside development is found in Fig. 4. Lupini et al. (1981) argued that the residual shear mechanisms are a function of particle packing. Hawkins and Privett (1985), Gibo et al. (1987) showed the relationship of ϕ_r with effective normal stress and reported that the residual friction angles are controlled by the effective normal stress as well as CF. At higher effective normal stresses, the difference $\phi_{r\ (0.5)}-\phi_{r\ (0.01)}$ is not significant due to a smoothened shear surface, compared to ϕ_r at lower effective normal stresses. On the other hand, the difference $\phi_{r\ (0.5)}-\phi_{r\ (0.01)}$ at lower effective normal stress, especially the negative values, could be explained in terms of shear mode depending on the plasticity characteristics and the difference of particle interlocking and the involvement of different types of particle behavior of non-platy particles in sand- and silt-dominated soils.

The absolute value of $\phi_{r\ (0.5)}-\phi_{r\ (0.01)}$ in Erdaocha1 (No. 1), Ikeda (No. 3), Tyunjun (No. 10), Chenyoulanxi (No. 13), Erdaocha2 (No. 14) and Miaowan3 (No. 15) at effective normal stresses less than or equal to 50 kN/m² are greater than 1.1°. The residual friction angles $\phi_{r\ (0.5)}$ and $\phi_{r\ (0.01)}$ of the Ikeda sample at 30 kN/m², being the maximum difference of 3.8° for the two different shearing rates among tested samples, are 14.2° and 18.0°, respectively. In practical terms, it would make a significant difference if ϕ_r of 14.2° or 18.0° is used in slope stability analysis.

Therefore, it is evident from these results that there is a tendency for having a greater effect of an increased shearing rate with decreasing effective normal stress. Hence, for the application of measured shear strength for stability analyses of shallow landslides, which are under low overburden pressures, it is important and advisable to measure the residual strength parameters of slip surface soils using the low shearing rate in a ring-shear test.

Summary and conclusion

In the present study, the influence of shearing rate on the residual strength parameter, ϕ_r, was investigated on landslide soil samples. The residual strength was obtained by ring-shear tests at two shearing rates (0.01 and 0.5 mm/min) under selected effective normal stresses. All tests were performed under the constant normal stress and drained condition. The landslide soil samples used in this study covered a wide range of soil types and properties, which included high and low plasticity soils as well as clay-rich and silt/sand-rich soil types. It was found that the residual friction coefficient, defined as τ_r/σ_n', under the lower effective normal stresses was higher than that under the higher effective normal stresses in all types of soil sample and at the two shearing rates. The relationships between the ϕ_r at two shearing rates and soil properties, such as liquid limit, plasticity index, and the clay fraction, showed that the $\phi_{r\ (0.01)}$ and $\phi_{r\ (0.5)}$ decreased with the increasing plasticity of soil samples. The difference in the ϕ_r at two shearing rates, $\phi_{r\ (0.5)}-\phi_{r\ (0.01)}$, under all effective normal stresses were either negative or positive values of which the maximum magnitude was generally about 1.0°. The relationships between $\phi_{r\ (0.5)}-\phi_{r\ (0.01)}$ and soil properties (LL, I_p, and CF) were not exhibited in a regular pattern. On the other hand, the $\phi_{r\ (0.5)}$ and $\phi_{r\ (0.01)}$ determined at each effective normal stress suggested that the tendency for increased negative effect of the ϕ_r with the decreasing effective normal stress was significantly exhibited in the slow shearing rate range. The absolute value of $\phi_{r\ (0.5)}-\phi_{r\ (0.01)}$ at lower effective normal stress was greater than 1.0°, with the maximum of about 4.0°. The negative shearing rate effect on ϕ_r at low effective normal stresses could be attributed to, and be affected by the undulating shear behavior due to poor or no slickenside development.

Acknowledgments

The authors sincerely acknowledge the assistance of M.S. Y. Eguchi of Graduate School of Agriculture, University of the Ryukyus (now at Ashikita-machi, Kumamoto prefecture) and Mr. T. Ganeko of Faculty of Agriculture, University of the Ryukyus (now at Okinawa prefecture), provided in support of the experimental program described in this paper.

References

ASTM D-6467 (2006) Standard Test Method for Torsional Ring Shear Test to Determine Drained Residual Shear Strength of Cohesive soils (ASTM D 6467-06a). ASTM, West Conshohocken

Bhat DR, Bhandary NP, Yatabe R (2013) Effect of shearing rate on residual strength of kaolin clay. Electron J Geotech Eng 18(G):1387–1396

Bishop AW, Green GE, Garga VK, Anderson A, Brown JD (1971) A new ring shear apparatus and its application to the measurement of residual strength. Geotechnique 21(4):273–328. doi:10.1680/geot.1971.21.4.273

Egashira K, Matsuo K, Gibo S, Nakamura S, Zhou Y, Inoue H, Sasaki K (2000) Clay mineralogical approach to the slip surface formation in the O'dokoro landlside, Niigata, Central Japan. Clay Sci 11:107–113

Gibo S (1994) Ring shear apparatus for measuring residual strength and measurement accuracy. J of the Jpn Landslide Soc 31(3):24–30 (in Japanese with English abstract)

Gibo S, Egashira K, Ohtsubo M (1987) Residual strength of smectite-dominated soils from the Kamenose landslide in Japan. Can Geotech J 24(3):456–462. doi:10.1139/t87-057

Gibo S, Egashira K, Ohtsubo M, Nakamura S (2002) Strength recovery from residual state in reactivated landslide soils. Geotechnique 52(9):683–686. doi:10.1680/geot.52.9.683.38837

Gibo S, Chen HH, Egashira K, Hayashi Y, Zhou Y (1997) Residual and recovery strength characteristics of soil from the reactivated landslide occurred at the National road across the middle part of Taiwan. J Jpn Landslide Soc 34(2):50–56 (in Japanese with English abstract)

Gibo S, Nakamura S, Kimura S, Chen C (2009) Characteristics of cross section and occurrence site of the first-activated type landslides in the area of Shimajiri-mudstone, Okinawa Island -For the risk evaluation of landslide-. J Jpn Landslide Soc 46(3):154–161 (in Japanese with English abstract)

Gibo S, Nakamura S, Sasaki K, Zhao T (2007) Shear strength characteristics and destabilization of the Erdaocha landslide, loess plateau, China. J Jpn Landslide Soc 40(4):156–161 (in Japanese with English abstract)

Grelle G, Guadagno FM (2010) Shear mechanisms and viscoplastic effects during impulsive shearing. Geotechnique 60(2):91–103. doi:10.1680/geot.8.P.019

Hawkins AW, Privett KD (1985) Measurement and use of residual shear strength of cohesive soils. Ground Eng 18(8):22–29

Holtz RD, Kovacs WD (1981) An introduction to geotechnical engineering. University of Michigan:88–89
Hungr O, Morgenstern NR (1984) High velocity ring shear tests on sand. Geotechnique 34(3):415–421. doi:10.1680/geot.1984.34.3.415
Japanese Geotechnical Society (2000) Explanation and method of the soil test. The Japanese Geotechnical Society: pp 441–545 (in Japanese)
Kanji MA (1974) The relationship between drained friction angles and Atterberg limits of natural soils. Geotechnique 24(4):671–674
Kimura S, Gibo S, Nakamura S, Vithana SB (2009) Shear strength characteristics of landslide soils, Asato landslide, Okinawa, Japan. Proc 19th (2009) Int Offshore and Polar Eng Conf, Osaka, Japan:156–161
La Gatta DP (1970) Residual strength of clays and clay-shale by rotation shear tests. Harvard Soil Mechanics Series (86). Harvard University, Cambridge
Lehane BM, Jardine RJ (1992) Residual strength characteristics of Bothkennar clay. Geotechnique 42(2):363–367
Lemos LJLJ, Skempton AW, Vaughan PR (1985) Earthquake loading of shear surfaces in slopes. Proc 11th Int Conf Soil Mech San Francisco 4:1955–1958
Lupini JF, Skinner AE, Vaughan PR (1981) The drained residual strength of cohesive soils. Geotechnique 31(2):181–213. doi:10.1680/geot.1981.31.2.181
Meehan CL, Brandon TL, Duncan JM, Tiwari B (2010) Direct shear testing of polished slickensided surfaces. Landslides 7(2):157–167. doi:10.1007/s10346-010-0199-7
Meehan CL, Tiwari B, Brandon TL, Duncan JM (2011) Triaxial shear testing of polished slickensided surfaces. Landslides 8(4):449–458. doi:10.1007/s10346-011-0263-y
Mesri G, Shahien M (2003) Residual shear strength mobilized in first-time slope failures. J of Geotech and Geoenviron Eng 129(1):12-31 doi: 10.1061/(ASCE)1090-0241(2003)129:1(12)
Nakamura S (2001) Studies on residual strength and strength recovery from residual state for landslide soils. PhD thesis, Kagoshima University, Kagoshima, Japan (in Japanese with English abstract)
Nakamura S, Gibo S (2000) The recovered strength of landslide soils and its relation to the effective normal stress. J of the Jpn Landslide Soc 37(3):18–24 (in Japanese with English abstract)
Nakamura S, Gibo S, Egashira K, Kimura S (2010) Platy layer silicate minerals for controlling residual strength in landslide soils of different origins and geology. Geology 38(8):743–746. doi:10.1130/G30908.1
Nakamura S, Gibo S, Egashira K, Yoshinaga A (2000) Recovered strength of landslide soils and its relationship with mineralogical composition. J of the Jpn Landslide Soc 37(3):10–17 (in Japanese with English abstract)
Nakamura S, Gibo S, Kimura S, Vithana SB (2011a) Average shear strength parameters along the slip surface of various types of landslides—Shimajiri-mudstone landslide, Okinawa. J of the Jpn Landslide Soc 48(5):9–20 (in Japanese with English abstract)
Nakamura S, Gibo S, Hayashi Y (2004) Tree-dimensional stability analysis procedure in which the residual factor is incorporated—an example of the Tyunjun landslide, Okinawa, Japan. Trans of JSIDRE 229:47–53 (in Japanese with English abstract)
Nakamura S, Gibo S, Zhou Y, Egashi K (1999) Determination of parameters for curved residual strength envelopes of landslides soils. J of the Jpn Landslide Soc 36(1):28–34 (in Japanese with English abstract)
Nakamura S, Kimura S, Eguchi Y, Vithana SB (2011b) Relationship between residual strength and specific surface area in landslide soils of different origins and geology. Proc 50th Conf the Jpn Landslide Soc, 30 Aug-2 Sep, Shizuoka:108-109 (in Japanese)
Skempton AW (1964) Long-term stability of clay slopes. Geotechnique 14(2):77–101. doi:10.1680/geot.1964.14.2.77
Skempton AW (1985) Residual strength of clays in landslides, folded strata and the laboratory. Geotechnique 35(1):3–18. doi:10.1680/geot.1985.35.1.3
Stark TD, Choi H, McCone S (2005) Drained shear strength parameters for analysis of landslides. J of Geotech and Geoenviron Eng 131(5):575–588. doi:10.1061/(ASCE)1090-0241(2005)131:5(575)
Stark TD, Eid HT (1994) Drained residual strength of cohesive soils. J of Geotech and Geoenviron Eng 120(5):856–871
Stark TD, Eid HT (1997) Slope stability analyses in stiff fissured clays. J of Geotech and Geoenviron Eng 123(4):335-343 doi: 10.1061/(ASCE)1090-0241(1997)123:4(335)
Sun B, Gibo S, Sasaki K, Zhao T, Nakamura S (2004) Classification on the basis of position of slip surface and features of loess landslides in the Southern Ningxia Hui Nationality Municipality, China. J Jpn Soc Nat Disaster Sci 23–1:79–92 (in Japanese with English abstract)
Suzuki M, Umezaki T, Kawakami H, Yamamoto T (2000) Residual strength of soil by direct shear test. J of Geo Eng 645/Ш-50:37-50 (in Japanese with English abstract)
Tika TE (1999) Ring shear tests on a carbonate sandy silt. Geotech test J 22(4):342–355
Tika TE, Hutchinson JN (1999) Ring shear tests on soil from the Vaiont landslide slip surface. Geotechnique 49(1):59–74. doi:10.1680/geot.1999.49.1.59
Tika TE, Vaughan PR, Lemos LJLJ (1996) Fast shearing of pre-existing shear zones in soil. Geotechnique 46(2):197–233. doi:10.1680/geot.1996.46.2.197
Tiwari B, Marui H (2005) A new method for the correlation of residual shear strength of the soil with mineralogical composition. J of Geotech and Geoenviron Eng 131(9):1139–1150. doi:10.1061/(ASCE)1090-0241(2005)131:9(1139)
Toyota H, Nakamura K, Sugimoto M, Sakai N (2009) Ring shear tests to evaluate strength parameters in various remoulded soils. Geotechnique 59(8):649–659. doi:10.1680/geot.8.029.3671
Vithana SB, Nakamura S, Gibo S, Kimura S (2012a) Correlation of large displacement drained shear strength of landslide soils measured by direct shear and ring shear devices. Landslides 9(3):305–314. doi:10.1007/s10346-011-0301-9
Vithana SB, Nakamura S, Kimura S, Gibo S (2012b) Effects of overconsolidation ratios on the shear strength of remoulded slip surface soils in ring shear. Eng Geolo 131–132:29–36. doi:10.1016/j.enggeo.2012.01.015
Wang G, Suemine A, Chen G (2010a) Residual shear behavior of serpentinite in Shiraishi landslide, Tokushima Prefecture and sliding mechanism. J of the Jpn Landslide Soc 47(5):265–273 (in Japanese with English abstract)
Wang G, Suemine A, Schulz WH (2010b) Shear-rate-dependent strength control on the dynamics of rainfall-triggered landslides, Tokushima Prefecture, Japan. Earth surf process and landforms 35:407–416. doi:10.1002/esp.1937
Yamaguchi (ed.) (1980) Landslides in Japan. Tokyo. The Japanese Society of Landslide and National Conference of Landslide Control
Yatabe R, Yagi N, Enoki M (1991) Ring shear characteristics of clays in fractured-zone-landslide. J of Geo Eng 436/Ш-16:93–101 (in Japanese with English abstract)
Yokota K, Yatabe R, Yagi N (1995) Strength characteristics of weathered serperntine. J of JSCE 529:155–163
Yokota K, Yatabe R, Yagi N (1997) Mineralogical and soil mechanical characteristics of landslides at serperntinite belt. J of JSCE 568:125–132
Zhou Y, Gibo S, Egashira K, Fujimoto M (1997) Physical and mineralogical properties and shear strength characteristics of soils from the landslides along the Min Jiang and the Zagunao He, China. Trans of JSIDRE 187:23–29 (in Japanese with English abstract)

S. Kimura · S. Nakamura (✉) · S. B. Vithana · K. Sakai
Faculty of Agriculture,
University of the Ryukyus,
Senbaru 1, Nishihara 901-0213, Okinawa, Japan
e-mail: s-naka@agr.u-ryukyu.ac.jp